Atmos. Meas. Tech., 6, 251–262, 2013
www.atmos-meas-tech.net/6/251/2013/
doi:10.5194/amt-6-251-2013

Atmospheric Measurement Techniques
Open Access

A centrifugal ice microtome for measurements of atmospheric CO_2 on air trapped in polar ice cores

B. Bereiter[1,2], **T. F. Stocker**[1,2], **and H. Fischer**[1,2]

[1]Climate and Environmental Physics, Physics Institute, University of Bern, Sidlerstrasse 5, 3012 Bern, Switzerland
[2]Oeschger Centre for Climate Change Research, University of Bern, Bern, Switzerland

Correspondence to: B. Bereiter (bereiter@climate.unibe.ch)

Received: 12 September 2012 – Published in Atmos. Meas. Tech. Discuss.: 26 October 2012
Revised: 29 January 2013 – Accepted: 30 January 2013 – Published: 7 February 2013

Abstract. For atmospheric CO_2 reconstructions using ice cores, the technique to release the trapped air from the ice samples is essential for the precision and accuracy of the measurements. We present here a new dry extraction technique in combination with a new gas analytical system that together show significant improvements with respect to current systems. Ice samples (3–15 g) are pulverised using a novel centrifugal ice microtome (CIM) by shaving the ice in a cooled vacuum chamber (−27 °C) in which no friction occurs due to the use of magnetic bearings. Both, the shaving principle of the CIM and the use of magnetic bearings have not been applied so far in this field. Shaving the ice samples produces finer ice powder and releases a minimum of 90 % of the trapped air compared to 50 %–70 % when needle crushing is employed. In addition, the friction-free motion with an optimized design to reduce contaminations of the inner surfaces of the device result in a reduced system offset of about 2.0 ppmv compared to 4.9 ppmv. The gas analytical part shows a higher precision than the corresponding part of our previous system by a factor of two, and all processes except the loading and cleaning of the CIM now run automatically. Compared to our previous system, the complete system shows a 3 times better measurement reproducibility of about 1.1 ppmv (1σ) which is similar to the best reproducibility of other systems applied in this field. With this high reproducibility, no replicate measurements are required anymore for most future measurement campaigns resulting in a possible output of 12–20 measurements per day compared to a maximum of 6 with other systems.

1 Introduction

In order to reconstruct past atmospheric CO_2 concentrations several studies analysed Antarctic ice cores, which contain small samples of the past atmosphere (e.g. Lüthi et al., 2008; Ahn and Brook, 2008; Bereiter et al., 2012) enclosed in air bubbles in the ice. The methods used in these analyses required several decades of development to reach an accuracy better than 5 % (Coachman et al., 1956; Neftel et al., 1982; Indermühle et al., 1999; see Bereiter, 2012, for the detailed history). One of the keys in these methods is the way how the air is extracted from the ice. During the extraction of air from ice samples several effects may alter the measured CO_2 concentrations: dissolution of CO_2 and carbonate chemical reactions in liquid water (Kawamura et al., 2003), adsorption/desorption effects at surfaces (Zumbrunn et al., 1982), contamination associated with mechanical friction in the extraction device (Lüthi, 2009), contamination associated with organic and inorganic substances in the ice (Anklin et al., 1995; Tschumi and Stauffer, 2000), and contaminations generally occurring in high vacuum applications.

Air extraction techniques for ice samples use three different basic principles to release the air from the ice: melting of the ice, sublimation of the ice, and mechanical pulverisation of the ice under dry conditions (referred to as dry extraction). The melt extraction has only shown limited success in CO_2 analysis due to possible chemical reactions taking place in the presence of liquid water (Kawamura et al., 2003); however, this principle is successfully used for the analysis of other gases in ice cores (e.g. Baumgartner et al., 2012; Schilt et al., 2010). The sublimation and dry extraction principles both provided reliable and reproducible CO_2 reconstructions.

One example is Siegenthaler et al. (2005) who applied both techniques. In terms of quantity, the dry extraction principle has produced many more CO_2 data because this technique has been applied for many years and because it requires less time for the extraction process resulting in a much higher sample throughput compared to sublimation systems. The fastest and most precise sublimation system to date currently has a sample throughput of 2 samples per day (Schmitt et al., 2011), whereas the fastest dry extraction system can analyse 16 samples per day (Bereiter et al., 2012). This limits the application of sublimation systems for larger measurement campaigns and represents a strong advantage for any dry extraction principle.

However, in terms of the quality of the extraction, the dry extraction technique has a clear disadvantage. Existing dry extraction devices release only 60 %–90 % and 50 %–80 % of the enclosed air in pure bubble ice and in pure clathrate ice, respectively (Schaefer et al., 2011; Sowers and Jubenville, 2000; Lüthi et al., 2010; Ahn et al., 2009), whereas sublimation extracts 100 % of the enclosed air from all ice types. In the bubble to clathrate transition zone (BCTZ) of ice cores (depth zone in ice cores where bubbles and clathrates coexist and where a fractionation of CO_2 concentration in clathrates relative to bubbles occurs) this leads to offsets between different extraction techniques depending on their extraction efficiencies for the two ice types (Lüthi et al., 2010; Schaefer et al., 2011). For this reason none of the current dry extraction systems provide accurate CO_2 data within the BCTZ, whereas the sublimation extraction overcomes this limitation (Lüthi et al., 2010). Among the dry extraction devices, the "ball mill" shows the smallest difference in extraction efficiency between bubble and clathrate ice of only 10 % which leads to more reliable results within the BCTZ in comparison with the cracker principle (Schaefer et al., 2011).

Further disadvantages with respect to the quality of the extraction are that the effects of adsorption and desorption of laboratory air at the inner surfaces (Zumbrunn et al., 1982) and that the effects of friction within the device (Lüthi, 2009) are more problematic in mechanical dry extraction systems than in sublimation systems. This is mainly due to the fact that stainless steel is used in dry extraction vessels compared to glass used for sublimation and that no moving parts are required in sublimation systems. In the needle cracker system previously used in our lab, we corrected for these effects by measuring during a day several gas-free single-crystal ice samples to which a standard gas is added (the correction varies between 2–8 ppmv depending on the day and history of the system). While this procedure provides sufficiently accurate results for CO_2 concentrations, it is, however, very challenging to control these effects for the more sensitive analysis of isotopes in CO_2 (Elsig, 2009).

Due to the constraints of the current dry extraction systems, we have developed a new dry extraction device with the following aims:

a. maximum possible extraction efficiency;

b. minimum mechanical friction within the device;

c. minimized inner area of the device that is exposed to ambient air during sample loading;

d. maximum possible sample throughput.

In addition to a completely new extraction device, we have also built a new gas analytical part for three reasons: (i) our original setup is based on the infrared laser spectrometer (IRLSM) of Lehmann et al. (1977) and has reached its lifetime; (ii) commercial optical gas analysers with sufficient reliability have become available (e.g., from Los Gatos Research, LI-COR or Picarro) and (iii) the new analysers can be embedded into an automated control environment.

2 Instrumental setup

2.1 Extraction device

The diameter of air clathrates in polar ice cores lies between 20–200 microns (Uchida et al., 2011). To open all enclosures and, hence, to reach maximum extraction efficiency with dry extraction, the ice sample must be pulverised to grain sizes smaller than the diameter of the enclosures. In the ice powder produced by our needle cracker, more than 90 % of the grains are larger, reaching up to several mm in diameter (see Fig. 3) explaining the low extraction efficiency of only 50 %–70 % (Lüthi et al., 2010). Other dry extraction principles show similar extraction efficiencies (Sowers and Jubenville, 2000; Schaefer et al., 2011). We examined alternative methods and found that the principle of shaving the ice has very high potential for fine pulverisation.

The design of the new dry extraction device is shown in Fig. 1. The sample holder (B) with a bay for the ice sample (A) is contained in a mantle (C) (diameter of B: 10 cm; tolerance between B and C: 1 mm). At the bottom of the mantle a fixed knife (D) is positioned such that it slightly protrudes into the interior. By rotating the sample holder anti-clockwise (arrows) with a frequency of up to 2000 rotations per minute, the ice sample gets pushed towards the inner mantle surface due to the centrifugal force and a layer of ice gets shaved off once per revolution when passing over the knife. The produced ice powder accumulates in the lower storage reservoir (E). The sample holder is rotated in the device until the sample is consumed and all ice is turned into ice powder, which is recognised acoustically when the noise originating from the impact of the sample on the knife stops. Our experiments showed that indeed ice samples have been quantitatively consumed at this point. The pulverisation principle of this new dry extraction device – called centrifugal ice microtome (CIM) – has not yet been applied in ice core research.

The amount of ice that gets shaved off the sample per cycle and the grain size of the resulting powder, respectively,

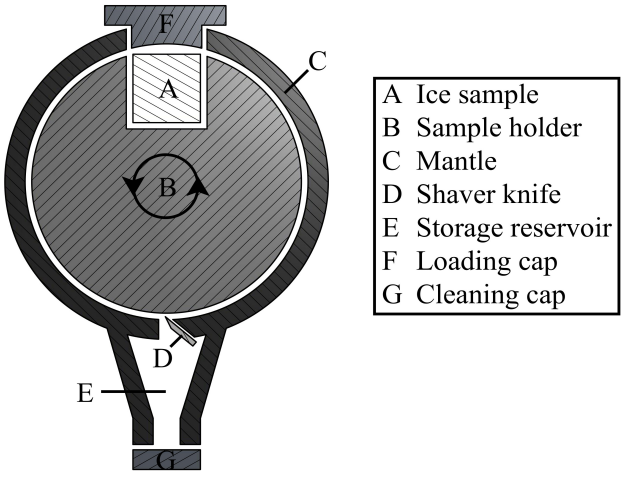

Fig. 1. Schematic illustration of the CIM for extracting enclosed air in ice under dry conditions. The legend and letters mark the different parts of the device including the sample (A). The sample holder (B) can be rotated within the mantle (C) as indicated by the arrows (tolerance between A and C: 1 mm). Access to load the sample holder is provided via the upper cap (F) and to remove the ice powder from the storage reservoir (E) via the lower cap (G).

is determined to first order by the distance between the inner mantle surface and the knife edge. Hence, the extraction efficiency can be optimized by adjusting this distance. The sample holder levitates and rotates contact free within the mantle using two magnetic bearings from Levitronix at each side of the sample holder. Levitronix systems combine the contact-free magnetic levitation and the rotation actuator in one device. The whole CIM is cooled down to $-27\,^{\circ}C$ to avoid any ice melting. This is achieved by placing the CIM inside an insulated box in which liquid nitrogen is evaporated in a controlled way. Besides the cooling effect this also provides a pure nitrogen atmosphere around the CIM which leads to lower measured CO_2 concentrations if the CIM leaks. This helps to distinguish effects that would increase the CO_2 concentration (i.e. leaks outside the CIM, adsorption/desorption of laboratory air at the inner surfaces of the device; Zumbrunn et al., 1982) from CIM leaks.

The sample holder is loaded through the access at the upper cap (F, CF flange sealing), and the ice powder is removed through the access at the lower cap (G, Swagelok VCR sealing). During loading and removing of the ice, the inside of the device is flushed with pure nitrogen to avoid contamination of the inner surfaces of the mantle with ambient air. In order to minimize the contamination of the cap inner surfaces during opening, their dimensions are kept as small as possible. Furthermore, the caps are placed in a dewar over a liquid nitrogen layer at the bottom of the dewar when they are not connected to the device. The constantly evaporating nitrogen in the dewar provides a cold and ambient air-free atmosphere for the caps.

The dimensions of the bay in the sample holder and the volume of the storage reservoir determine the possible sample sizes with which the CIM can be loaded. In the current realisation sample masses of up to 15 g can be accommodated. The mantle of the CIM can be split into two pieces (indium sealing) such that the complete sample holder can be replaced. With a redesigned sample holder a maximum sample mass of 40 g could be realised. For larger samples a complete redesign of the CIM would be required, but upscaling of the extraction principle is possible. The whole construction of the CIM is made up of stainless steel with the exception of the material for the knife (titanium) and for the casing at the magnetic bearings where an insulator is required to allow for the magnetic levitation to work (here we use glass which is connected to the stainless steel parts using indium sealing).

2.2 Gas analytical part

The setup of the complete system is shown in Fig. 2. Four main parts constitute this system: the new extraction device (red circle), an adjustable volume using a membrane bellow (dashed rectangle), the optical gas analyser LI-7000 from LI-COR (green rectangle) and the standard gas containers (STD 1–3). Both the LI-7000 and the CIM are placed in a temperature stabilizing box. The box around the LI-7000 consists of wood panels, thermal insulation and a piezoelectric cooler element to keep the device at stable room temperature within $\pm 0.02\,^{\circ}C$ during a measurement day (peak to peak). Larger variations in the order of $\pm 0.1\,^{\circ}C$ deteriorate the measurement accuracy. The box around the CIM is needed for cooling the CIM down to $-27\,^{\circ}C$.

The optical gas analyser LI-7000 (LI-COR, 2005) uses the non-dispersive infrared (NDIR) measurement technique which is a less sensitive technique than used for our original IRLSM and other commercial optical gas analysers (i.e. of Los Gatos Research, Baer et al., 2002; Picarro, Crosson, 2008). However, the NDIR technique is less complex and thus robust, and the device is small and less expensive than other devices. It also allows us to access the raw data for subsequent processing. By stabilizing the ambient temperature of the LI-7000 (see above) and using a relatively long integration time for the measurement data (up to 6 min), the precision of the LI-7000 can be increased to a level sufficient for this application (Bereiter, 2007).

In order to understand the role of the different parts of the system, the measurement procedure is described here: the whole measurement system including the CIM is evacuated in the beginning. After disconnecting the CIM from the vacuum system and connecting it with the nitrogen flush, the CIM is loaded with a sample and reconnected to the vacuum system for a few minutes in order to let the sample surfaces sublimate and, thus, remove possible surface contaminations. Then the valves leading to the CIM are closed and the rotation of the sample holder is started. During the rotation for roughly one minute, the ice sample is completely turned into

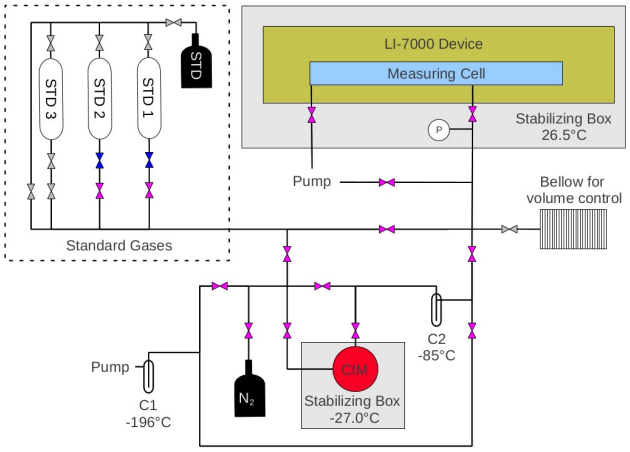

Fig. 2. Schematic illustration of the complete system for CO_2 measurements on polar ice cores. Red circle: CIM (details in Fig. 1); green rectangle: LI-7000 optical CO_2 analyser from LI-COR with its measurement cell (blue); hashed rectangle: adjustable volume using a membrane bellow (stainless steel); dashed rectangle: standard gas unit with three standard gas reservoirs (STD 1-3); grey squares: temperature stabilizing boxes used for the LI-7000 and the CIM; C1 and C2: cold traps; *P*: pressure gauge; pink valves: pneumatically actuated diaphragm valves; blue valves: pneumatically actuated full-metal bellow valves; grey valves: manually actuated full-metal bellow valves. The ends of the vacuum line marked with a pump are connected to vacuum pumps. All vacuum valves and fittings are made of stainless steel and manufactured by Swagelok.

ice powder and the air is released from the ice. The released air is then expanded towards the membrane bellow passing cold trap C2 (−85 °C) which collects water vapour. For this expansion two different options have been tested in order to determine system artefacts: first, direct expansion into the membrane bellow; second, two step expansion first to C2 and then to the membrane bellow. For the second option, different waiting times between the first and second step of up to 5 min have also been tested (see Sect. 3.3 for further details).

Independent of the option applied, the membrane bellow is expanded to its maximum volume during the connection with the CIM in order to transfer as much sample air into the bellow as possible. Afterwards, the valves between the bellow and the CIM are closed and opened towards the measuring cell. Then, the volume of the bellow is reduced to its minimum volume in order to push as much air as possible into the LI-7000 measuring cell. In this way, 2.3 times more air can be transferred to the measuring cell in comparison to the case when the air would be expanded directly into the measuring cell without the use of the membrane bellow.

After closing the valves leading to the LI-7000, the operating computer starts to record the infrared absorption signals from the LI-7000 while the rest of the system is evacuated again. When the detection is finished, the sample air is pumped out of the LI-7000 measuring cell which is then reloaded with standard gas from one of the standard gas containers. During this procedure, the pressure in the cell – measured by pressure gauge *P* – is adjusted to the pressure of the previous sample by adjusting the volume of the membrane bellow (deviation between the two pressures within 1.5 per mill). The concentration of the sample air is calculated on the operating computer using the recorded raw infrared signals from the LI-7000 of both gases (sample and standard gas). Since temperature and pressure are equal for the sample and the standard, the sample concentration is directly proportional to the ratio of the two measured absorption signals. The system control is based on LABView and routine measurements are performed automatically. All processes run automatically except loading and removing of the ice sample.

3 Results and discussion

3.1 Ice powder characteristics

The extraction efficiency is determined by the grain size of the produced ice powder. In Fig. 3 grain size distributions from ice powders produced with the cracker and CIM device used in our lab are compared. The distributions have been determined in the following way: a dewar was cooled down and filled with dry ice powder in order to keep the dewar cool. Artificially produced gas-free single-crystal ice was pulverised in the device. This showed no visual difference to powder from real polar ice and the produced powder was filled into the dewar. The ice/dry ice powder mixture was then filled in a sieve tower (sieves from Fritsch and Retsch, Shaking table from Fritsch) located in a cold room (−15 °C) in order to separate the different grains from the ice powder. After shaking the sieve tower for about 5 min the powder was left to let the dry ice sublimate so that only the ice powder remained. Then, the masses of the collected ice powder on the different sieves were measured.

There is a clear difference between the grain size distribution of the cracker and the CIM. In the cracker powder about 2/3 of the ice mass contains grains with sizes above 1 mm. In the CIM powder less than 1/4 of the ice mass falls into this category. This large amount of coarse grains in the cracker powder explains both the extraction efficiency of only 50 %–70 % (depending in the ice characteristic) and the preferential extraction of air from the large enclosures (Lüthi et al., 2010). About 1/3 of the ice powder mass from the CIM has grain sizes between 1 mm and 0.5 mm and about 1/2 between 0.5 mm and 0.1 mm. Even smaller grain sizes are negligible in both principles, however, it is notable that the small grain sizes below 0.25 mm are very sticky and can form clusters of grains that no longer pass the sieves anymore. Hence, it might be that more smaller grains exist but are not recorded with this procedure.

With the CIM, a setup for “coarse” and one for “fine” ice powder has been tested by adjusting the knife position (Fig. 3, dark and light grey bars). The setups differ

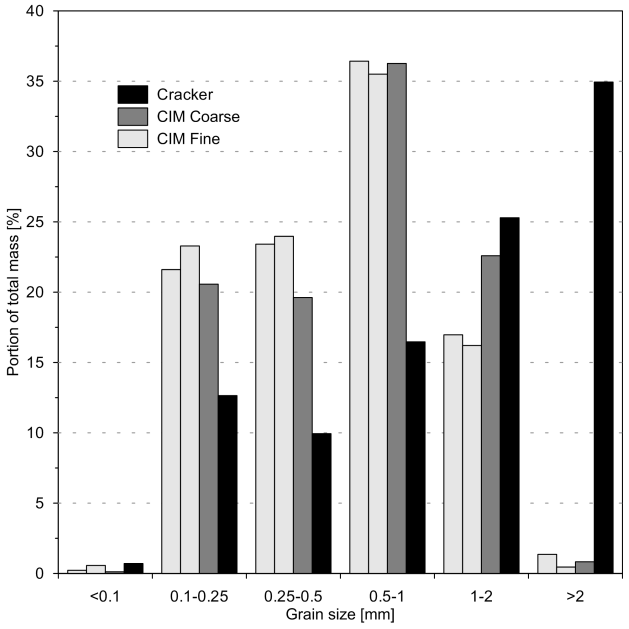

Fig. 3. Grain size distribution of the ice powder produced with the cracker and CIM used in our lab. The height of the bars represents the percentage of the total powder mass found in a specific grain size range. The black bars indicate powder from the cracker (total mass: 16 g), the grey bars from the CIM with two different knife positions producing coarser (dark grey) and finer (light grey) powder. With the fine setup two experiments have been performed (total mass for each CIM experiment: 9.5 g).

particularly in the amount of larger grains. The mass of the powder produced with the coarse setup consists to 23 % of grains above 1 mm, whereas the powder produced with the fine setup contains only 17.5 % of the mass in this size range. The two equal experiments with the fine setup reproduce this result within 1.5 % indicating that this difference is clearly significant. The missing mass of larger grains is found between 0.5 mm and 0.1 mm while the amount between 1 mm and 0.5 mm seems to be roughly equal for the coarse and fine setup. With this size distribution also the CIM will not extract 100 % of the trapped air in clathrated ice since the diameter of clathrates in polar ice cores lies between 0.02–0.2 mm (Uchida et al., 2011). It is difficult, however, to quantitatively calculate an efficiency from this distribution since the produced grains as well as the enclosures consist of different geometries which would need to be known for such a calculation. For a more quantitative estimate of the extraction efficiency real ice core measurements were used as described in Sect. 3.4. Nevertheless, the sieving results suggest that the extraction efficiency is higher with the CIM compared to the cracker. For the issues within the BCTZ associated with the extraction efficiency (Lüthi et al., 2010) the difference between the efficiency within bubble and clathrate ice is the crucial determining factor and not necessarily the absolute value of the efficiencies. This difference can only be quantified by measurements within the BCTZ (see Fig. 7).

In order to derive the grain size distributions of the CIM shown in Fig. 3, one single ice sample of about 9.5 g has been shaved, whereas for the cracker distributions the powder of 3 samples has been collected accumulating to about 16 g of ice. The reason for this is that the cracker does not crack the samples equally well and therefore several samples needed to be averaged. In contrast to that, the CIM shows a constant pulverisation characteristic from one sample to the other as indicated by the two equal experiments with the fine setup. This suggests that the extraction efficiency from one sample to the other is also more constant with the CIM than with the cracker. This is a further advantage for measurements within the BCTZ. Furthermore, the CIM pulverises all sample sizes from very small pieces (less than 1 g) up to the maximum size (about 15 g) and even fractured ice samples to powder with similar characteristics as seen in Fig. 3. This is not the case with our cracker and cracker systems of other laboratories (Ahn et al., 2009). In the needle cracker, besides the geometry of the needle matrix, also the distance over which the needles can accelerate until they hit the ice and to what extent the ice powder fills the sample chamber are important for the quality of the pulverisation. Hence, with the cracker principle different sample dimensions result in different extraction efficiencies, whereas the extraction efficiency of the CIM is much less dependent on the sample sizes.

3.2 Results from air standards

The accuracy of the gas analytical part of the system is investigated in a first step with standard gas measurements (standard gas is measured against itself). To the first order, the deviation of these measurements depends on the stability of the system which is determined by the temperature of the LI-7000 (see Sect. 2.2). To the second order, the deviation depends on the pressure of the sample (sample amount) at which the measurements are performed as well as on the CO_2 concentration of the gases. With a stable system, a standard deviation of 1.2 ppmv (1σ) is achieved for the worst case of low concentration (197.62 ppmv) and low pressure (4 mbar). This represents already a significant improvement over the previously used infrared laser spectrometer (IRLSM) (1.7 ppmv). In the case of higher concentration (251.63 ppmv) and high pressures (10 mbar) a standard deviation of only 0.4 ppmv is reached (Siegrist, 2011).

The measurements presented in this work (Figs. 4–7) are performed under conditions at which the standard deviation of the gas analytical part lies at 1 ppmv or lower. This is about a factor 2 lower than the standard deviation of the IRLSM. As mentioned in Sect. 2.2, the NDIR technique used in the LI-7000 is much less sensitive to CO_2 compared to the IRLSM technique, however, this is overcompensated by the longer integration time of the infrared signals, the better stability and the automation of the new system. Due to the relatively

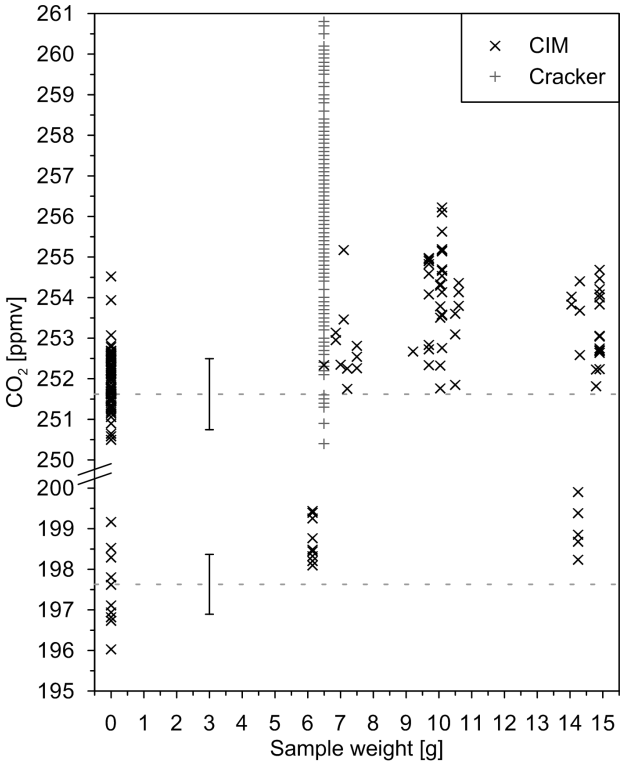

Fig. 4. Measurement results of the CIM system (black crosses) and cracker system (grey crosses) using standard gas with 251.62 ppmv (upper dashed line) and 197.63 ppmv (lower dashed line) CO_2 concentration and gas-free single-crystal ice samples. In the case of the CIM different sample weights have been used. For both standard gases an error (1σ) for the single CIM data point is given by the error bars initiated at 3 g sample weight (SIO197: ± 0.74 ppmv SIO251 $\pm$ 0.88 ppmv). They represent the standard deviations of all data points of the corresponding standard gas shown in this figure. To calculate these deviations, in a first step all results from samples with weights > 0 were corrected for their mean offset to the corresponding standard value.

long time needed for the whole process of cleaning, loading and evacuating of the CIM as well as the subsequent extraction, the integration time of the infrared absorption system (up to 6 min) is not a limiting factor with respect to sample throughput.

3.3 Results from gas-free ice

First, measurements with gas-free ice are presented using artificially made single-crystal ice. In terms of the procedure, the only difference to real ice core samples is that before the shaving process gets started, a standard gas is added to the CIM. With these types of measurements system artefacts can be investigated. For all the results discussed in this section and shown in Figs. 4 and 5, the CIM was adjusted to produce "coarse" powder (see Fig. 3). No difference has been found between the two settings for these type of measurements.

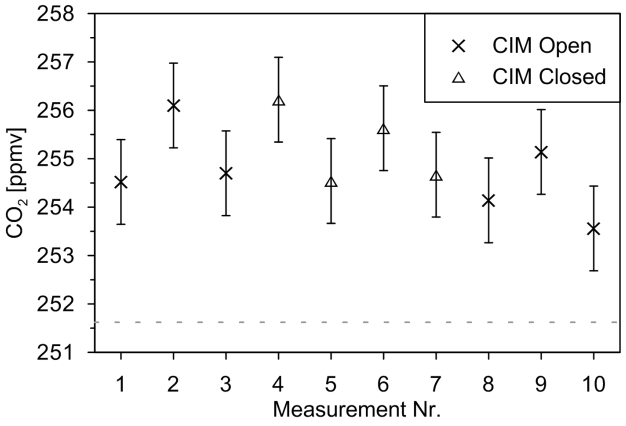

Fig. 5. Measurement results of the CIM system of one day using standard gas with 251.62 ppmv CO_2 concentration and gas-free single-crystal ice samples. Crosses represent measurements during which the CIM was opened and the ice was shaved. Triangles show measurements where the CIM was loaded with ice but was kept closed and no ice was shaved. The error bars are equal to the error bar in Fig. 4 for SIO251.

Figure 4 shows the results of single-crystal measurements using two different standard gases from the Scripps Institute of Oceanography (197.63 ppmv, SIO197; 251.62 ppmv, SIO251) and different weights of single-crystal ice samples. The results with SIO197 (bottom section) show no offset when running the whole process without ice (0 g sample weight). However, when the CIM is loaded with ice, an offset between the reference value (dashed line) and the results of 1.19 ± 0.15 ppmv (1σ) is found on average. There is no indication for a weight dependency in these data which suggests that the offset is independent from the amount of ice shaved. The general pattern of the results with SIO251 (top section in Fig. 4) is the same: (i) larger offset to the reference value when using ice compared to the results without ice; and (ii) no weight dependency. However, these data show a larger spread compared to SIO197 (see the error bars in Fig. 4 and the explanation in the figure caption) and there is a tendency to a positive offset without ice. The reason for this is that all measurements with SIO197 have been performed with the same procedure and only the weights of the samples have been changed. For the measurements with SIO251, in addition to the weights the options of how the extracted air is expanded into the measuring cell have also been varied (see Sect. 2.2). During some measurements the air has been immediately expanded towards the measuring cell after the shaving process has been finished (i.e. no delay in the process). During others a waiting time of up to 5 min has been introduced between the end of the shaving process and the expansion of the air. In addition, during this waiting time in some cases the CIM was closed while in the others the CIM stayed connected to the cold trap C2.

During all SIO197 measurements, the air has been immediately expanded towards the measuring cell. This is the optimal case since the potential for contamination caused by desorption of CO_2 from the inner surfaces of the CIM (Zumbrunn et al., 1982) and the risk of leakage effects in the CIM is minimized. For the SIO251 measurements without ice, performed under the same optimal conditions, no offset to the reference value was found (as was the case for the corresponding SIO197 measurements). The offset increased to 0.6 ppmv when a waiting time of 5 min was introduced. There was no clear change found whether or not the CIM was connected to the cold trap during the waiting time, however, if at all we would expect an increase of the offset due to the water vapour flux from the CIM to the trap preferentially transporting CO_2 (Stauffer and Oeschger, 1985).

The different options of the expansion procedure have been introduced in order to account for slowly decaying clathrates. Therefore, for pure bubble ice the option of immediate expansion towards the measurement cell is used, whereas for (partly) clathrated ice (Figs. 6 and 7) the option with a waiting time is applied. The option of connecting the CIM to C2 or not during the waiting time did not influence the measurements on polar ice performed in this work. Since the different options have an influence on the system accuracy and precision, two cases from the measurements with gas-free ice are selected to provide a range of the system accuracy and precision. The best results so far have been obtained during a sequence of 14 single SIO197 measurements distributed over two days with direct expansion towards the cell. The mean value and the standard deviation of this sequence is 198.8 ppmv and 0.6 ppmv, respectively. The lower quality limit is given by the averaged values of all SIO251 measurement with any waiting time up to 5 min (8 days, 40 measurements; mean: 254.0 ppmv, standard deviation: 1.1 ppmv).

The single-crystal measurements performed with the cracker system (Fig. 4, grey crosses) show a much larger spread than the ones from the CIM system. The standard deviation of these data is 2.7 ppmv which is roughly three times larger compared to the CIM system. Furthermore, the average offset to the reference value with the cracker system is about 4.9 ppmv whereas with the CIM system this is only 2.0 ppmv (average over all SIO251 data excluding 0 g sample weight). A possible reason for the offset to the reference value in the cracker system is adsorption and desorption of laboratory air at the inner surfaces of the cracker (Zumbrunn et al., 1982).

Figure 5 shows single-crystal measurements with the CIM system of one single day during which two different sets of measurements have been performed: the set represented by the crosses followed the normal procedure where the CIM was opened to clean and load; for the set represented by the triangles the CIM was kept closed throughout the measurement, however, ice was present in the CIM to ensure the same water vapour pressure inside. The data show no

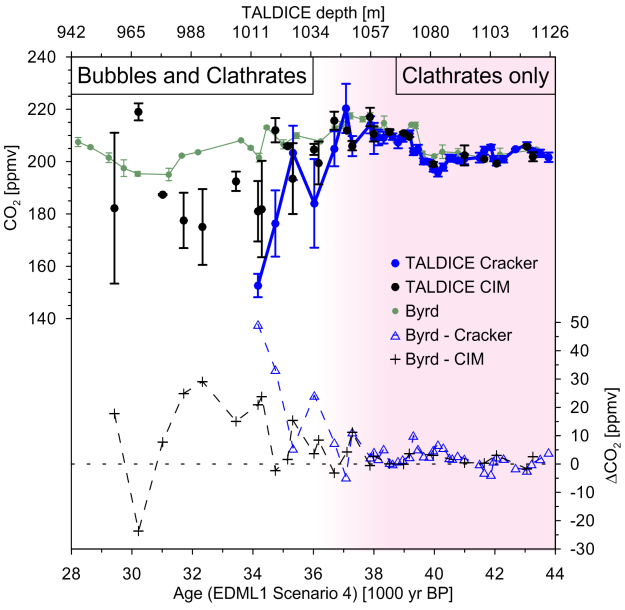

Fig. 6. Top: CO_2 concentrations derived with the CIM system (black dots, this study) and our cracker system (blue dots, Bereiter et al., 2012) using ice samples from the TALDICE core. In green, CO_2 data from the Byrd ice core are shown using an independent cracker system (Ahn and Brook, 2008). The records are synchronised onto the EDML1 Scenario 4 gas age scale (Ruth et al., 2007) according to Bereiter et al. (2012). Bottom: CO_2 concentration differences inferred between the different records of the top part using linear interpolation: blue triangles represent the differences between the green and the blue records; black crosses between the green and the black records. The white area represents the part of the TALDICE core located in the BCTZ, the pink area the fully clathrated ice. The Byrd ice core covers the entire time window in fully clathrated ice. All the CIM results are obtained with the CIM setting to produce "coarse" ice powder (see Fig. 3). The CIM data points with an error bar consist of two to six single measurements, those without a bar of only one.

significant difference between these two sets. This implies that the amount of CO_2 added to the sample air via adsorption of laboratory air at the inner surfaces during opening and desorption afterwards is negligible owing to the design of the CIM and the handling with the CIM caps during opening (see Sect. 2.1).

The two sets of Fig. 5 differ in a second point: in the first set the ice is shaved and, hence, friction occurs between ice and metal; in the second set no friction occurs since no ice is reloaded and the CIM stayed closed. The experiments of Lüthi (2009) with a prototype ice mill showed that the rotation of metallic or ceramic ball bearings inside the sample chamber can lead to strong CO_2 contamination of the sample air of up to 1000 ppmv. The results with different bearing materials and treatments of the bearings suggest that the source of the contamination is the friction within the bearings. Hence, the two different sets of Fig. 5 further show that

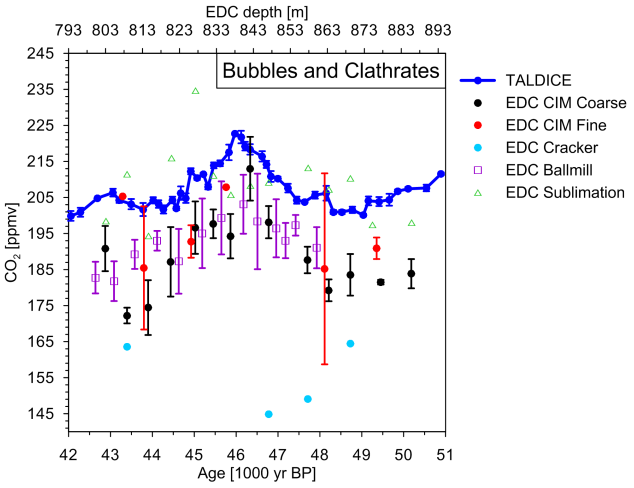

Fig. 7. CO_2 concentrations derived from the BCTZ of the EDC ice core with the CIM system (black and red dots, this study) and our cracker system (light blue dots, Lüthi et al., 2010) as well as with a system using the sublimation principle of Siegenthaler et al. (2005) (green triangles, Lüthi et al., 2010) and a ball mill (purple squares, Schaefer et al., 2011) to extract the air. As a reference, data from the fully clathrated ice of the TALDICE core are shown in dark blue (Bereiter et al., 2012) representing the atmospheric concentration. The TALDICE record is synchronised onto the EDML1 Scenario 4 gas age scale (Ruth et al., 2007) according to Bereiter et al. (2012). The EDC records are plotted on EDC3 Scenario 4 gas age scale (Parrenin et al., 2007) which is synchronised to the EDML1 age scale. For 6 CIM data points both the "coarse" (black) and the "fine" (red) CIM settings (see Fig. 3) were applied, whereas the red data points are shifted by 100 yr forward in time relative to the corresponding black data point for better visibility. The CIM data points with an error bar consist of two to four single measurements and the ones without a bar of only one.

the friction between the ice and the metallic casing is not problematic. We note, however, that CO_2 contamination of up to 10 ppmv has been found when using a hardened stainless steel for the knife for which reason we now use titanium.

In the case of the cracker system, single-crystal measurements were used to correct for the system artefacts in the following way: during a measurement day at least four single-crystal measurements were performed at regular intervals. From the linear regression through all these measurements, a correction value for the ice core samples – that have been analysed in between – is calculated. The single day measurement sequence of the new CIM shown in Fig. 5 illustrates two important features regarding this correction procedure. First, the average offset during one day stays stable with the CIM (standard deviation of all data in Fig. 5: 0.9 ppmv). Second, the mean offset during one day (here 3.3 ppmv) can be slightly different from the mean offset over several days (2.4 ppmv for this type of measurements). For these reasons corrections are applied only on the day they were determined. However, the question arises whether it is necessary to derive a daytime-dependent correction as done for the cracker data, or if a daily constant correction is sufficient. In Figs. 6 and 7, the data are corrected for the system artefact in a daytime-dependent way as for the cracker system. No difference is found so far compared to the simpler daily-mean correction. More data are needed to investigate this further.

3.4 Results from Antarctic ice cores

To test the system with real samples, ice from three different Antarctic ice cores has been used, each covering a different time window and representing different ice characteristics: (i) bubble ice from about 146 m depth of the Byrd ice core containing pre-industrial air; (ii) ice around the border between the BCTZ and pure clathrated ice of the Talos Dome ice core (TALDICE) covering the period between 34 000 and 44 000 yr BP (Fig. 6); and (iii) ice from the middle of the BCTZ of the EPICA Dome C ice core (EDC) covering the period between 45 000 and 55 000 yr BP (Fig. 7). The measurement procedure for the corresponding ice types is found in Sects. 2.2 and 3.3. All CIM data are offset corrected as described in Sect. 3.3. For each data point from the TALDICE and EDC core averages over two to four single measurements have been calculated. During a measurement day at least 12 single ice samples have been measured. Additionally, measurements with gas-free ice as described above have been performed at regular intervals to derive a correction for the system artefacts. All CIM results shown in Figs. 6 and 7 used the CIM setting to produce "coarse" powder (see Fig. 3) with the exception of 6 measurements on the EDC core using the "fine" setting (Fig. 7, red).

At the Byrd ice core five neighbouring ice samples have been cut from a depth of about 146 m containing pre-industrial air. One of these samples has been analysed with the sublimation system of Schmitt et al. (2011) and the other four with the CIM system, where two of the CIM samples were about 6.5 g and the other two 14.5 g. Sample weight for the sublimation system is about 30 g. The results from the CIM system (6.5 g: 284.5 ppmv, 285.8 ppmv; 14.5 g: 283.6 ppmv, 285.6 ppmv) show no sample-weight dependency as suggested from the single-crystal measurements. Furthermore, their mean and the corresponding 1σ error (284.9 ± 0.6 ppmv) indicates an insignificant difference to the result from the sublimation system (286.6 ± 2.0 ppmv; the error of the sublimation value corresponds to the system uncertainty given in Schmitt et al., 2011). This indicates that the CIM system is able to reconstruct atmospheric CO_2 concentrations using bubble ice.

The data from the TALDICE core (Fig. 6) show differences dependent on the ice characteristics. In the fully clathrated ice (pink part) the data from the CIM and the cracker system (Bereiter et al., 2012) show no offset between each other and also agree with the data from the Byrd ice core (Ahn and Brook, 2008) within a few ppmv. This suggests that the CIM system is also capable to reconstruct CO_2 using

fully clathrated ice. The data error within the fully clathrated ice of the TALDICE core is similar for the cracker and the CIM system. The average error of these measurements in the cracker data is at 1.2 ppmv (1σ) (Bereiter et al., 2012) and in the CIM data around 1.5 ppmv. Note, that in the latter case the value is based only on 10 data points in contrast to 110 data points in the former case, and that the ice in the latter case originates from just below the BCTZ, where more data scatter is observed (Lüthi et al., 2010; Bereiter et al., 2012). For the data points derived with the cracker system at least four single measurements are performed, whereas the data from the CIM system are based only on two to three measurements. At one ice core section in the fully clathrated part, eight neighbouring samples have been analysed with the CIM in order to derive the reproducibility in this type of ice. The standard deviation is 1.1 ppmv which is comparable to the reproducibility with gas-free ice and in the range of the system with the best reproducibility found in the literature so far (standard deviation between 0.9 and 1.5 ppmv, Ahn et al., 2009). Due to this good reproducibility, future measurement series with the CIM system on non-BCTZ ice might no longer require replicate measurements unless a data error below 1.5 ppmv is required.

In the BCTZ of the TALDICE core (Fig. 6, white part) the cracker and the CIM systems show significantly lower values compared to the Byrd record which covers the whole time window shown in Fig. 6 in fully clathrated ice. The difference to the Byrd record of both systems changes roughly between 1010 and 1055 m depth. Above 1010 m depth, the record of the CIM shows a rather constant offset of approximately 20 ppmv connected to a larger scatter of about 7 ppmv (average error above 1010 m depth) with one outlier being above the Byrd record. This offset is consistent with the one observed in the BCTZ of the EDC ice core (Fig. 7). This suggests that the offset is relatively constant throughout a large part of the BCTZ and that it is similar in different ice cores. The generally coarser and more variable sample pulverisation in the cracker (see Sect. 3.1), as well as the few cracker data in the BCTZ (see Fig. 7), suggest a much larger scatter in these data and an offset around 50 ppmv.

Further insight into the differences between different ice types and extraction techniques is obtained from the data shown in Fig. 7. This time window is located in the BCTZ of the EDC core, whereas in the TALDICE core this lies in the fully clathrated ice. The record from the TALDICE core (Bereiter et al., 2012) is used here as the reference record representing the effectively trapped CO_2 concentration. For the EDC ice core, CO_2 data from three different extraction techniques are available for this time window: four data points from our cracker system, 14 using an older sublimation extraction technique (Lüthi et al., 2010) and 13 data points using a ball mill for the gas extraction (Schaefer et al., 2011). The new data set from the CIM system shows lower values of about 20 ppmv on average compared to the TALDICE record similar to the offset in the BCTZ of Fig. 6. Since CO_2 is enriched in clathrates and depleted in bubbles in the BCTZ (Lüthi et al., 2010; Schaefer et al., 2011), these lower values imply that also the CIM technique preferentially extracts air from the bubbles compared to the clathrates in the BCTZ. The ball mill and the CIM data are on the same level on average and about 30 ppmv higher than the cracker data indicating that the former two techniques have similar characteristics with respect to the difference in extracting air from bubbles and clathrates in the BCTZ, and that the cracker technique shows the largest offset in this respect. This is in line with the finer pulverisation of the ice sample of the CIM compared to the cracker (Fig. 3). The data from the older sublimation extraction (Lüthi et al., 2010) analysed with the system presented in Siegenthaler et al. (2005) show no offset to the TALDICE record on average over the entire age range due to the 100 % extraction efficiency, however, a large scatter around the TALDICE data.

The EDC records from the CIM and the ball mill reproduce the general atmospheric evolution seen in the TALDICE record but with higher scatter and a significant offset to TALDICE. Neither the cracker nor the sublimation data (accuracy ± 2.0 ppmv, Siegenthaler et al., 2005) show the general atmospheric pattern. Lüthi et al. (2010) found strong CO_2 variations in the BCTZ within a few centimetres of the ice core that exceed both analytical uncertainties and possible entrapped climatic variations. They explain this by layer-wise formation of clathrates in the BCTZ leading to CO_2 increase in clathrate-enriched layers at the expense of the neighbouring layers. The cracker data are most affected from this effect because the ice samples have a small vertical extent along the ice core axis of 2.2 cm, well resolving these layers. Even though the vertical extent of the sublimation samples is about twice as much, the air released from these samples corresponds to a comparable vertical extent as the one from the cracker samples. This is due to the fact that the laser applied for the sublimation process in this specific system of Siegenthaler et al. (2005) points to the centre of the sample sublimating only about 1/3 of the total ice from the central region of the sample.

The vertical extent of the CIM samples is 3.2 cm, whereas most of the data points are mean values of two neighbouring samples covering together 6.4 cm of ice core length. The same is true for the ball mill data with a single sample extent of 4.5 cm and a total extent of 9 cm. Therefore, the data from the CIM and the ball mill are less affected from the clathrate layering in the BCTZ compared to the cracker and sublimation data and, hence, show less scatter. Note that Schaefer et al. (2011) found that the layer-wise formation can not explain all the scatter in the BCTZ data. The remaining scatter might originate from loss of air through cracks in this brittle ice which might also have an influence on the offset between the EDC and the TALDICE record. However, small offsets between CO_2 records from ice cores of a few ppmv have been found also in fully clathrated ice (Bereiter et al., 2012) which

are most likely related to inter-laboratory standardisation issues.

The CIM data shown in Fig. 7 represent 14 depth levels at which replicate measurements have been performed. At 6 out of these 14 depth levels replicates have been analysed applying both the "coarse" (black) and the "fine" (red) CIM settings. Within 5 of these 6 depth levels, the replicates using the "fine" setting show higher values of roughly 10 ppmv on average relative to the corresponding "coarse" results. This is in line with a higher extraction efficiency associated with the "fine" setting, opening more of the smaller clathrates which preferentially trap CO_2 at the expense of the bubbles in the BCTZ (Schaefer et al., 2011). The "fine" and the "coarse" setting differ in particular in the relative amount of grains produced larger than 1 mm (see Fig. 3) which suggests that these grains trap the "missing" CO_2. Future pulverisation optimisations of the CIM must therefore focus on minimisation of the amount of these larger grains rather than production of more small grains. The scatter within these "fine" analysis is comparable to the one of the "coarse" analysis. This issue can be further improved by a larger vertical extent of the samples.

Finally, the extraction efficiency of the CIM has been estimated based on nine single measurements from Figs. 6 and 7. With the pressure reached in the measuring cell during these measurements and the known volume of the different sections of the system, the released amount of air from the sample can be calculated. There are two main uncertainties that limit this estimate: first, the uncertainty of the air content of the original ice sample; second, the uncertainty of the water vapour pressure present in the CIM after air expansion. For the air content in the EDC samples, we use an average of the data of Raynaud et al. (2007) of the specific depth window (90 mL kg^{-1} STP); however, this represents the actual air content of the ice sample only within ± 2 %. For the air content in the TALDICE core a by-product of the CH_4 and N_2O measurements of Schilt et al. (2010) is used which indicates an air content of about 100 mL kg^{-1} in this section of the core; however, this estimate has an uncertainty of about ± 4 %. The uncertainty associated with the water vapour pressure is derived from the fact that the extracted air in the CIM is expanded into the membrane bellow and disconnected from the CIM within 20 s. It is unknown whether or not the water vapour pressure, which supersedes the extracted air in the CIM, reaches equilibrium in this short time. The resulting extraction efficiency is minimal if we assume that equilibrium is reached. Therefore, the uncertainty associated with the water vapour only allows us to infer a lower limit of the extraction efficiency. Taken together, a minimal extraction efficiency of about 90 % is estimated for fully clathrated ice. The estimates for the "fine" CIM setting tend to higher efficiencies by a few % compared to the "coarse" setting. Due to the mentioned uncertainties, however, a significant difference can not be determined. Note, that also 100 % extraction efficiency lies within the range of this estimate; however, the grain size distribution and the measurements in the BCTZ suggest that a small fraction of the trapped air is not released.

4 Conclusion and outlook

The new dry extraction technique for atmospheric CO_2 reconstructions from polar ice cores presented here shows significant improvements compared to the technique used hitherto in our institute (cracker) and other dry extraction principles. The new CIM principle pulverises the ice samples more homogeneously and to finer powder. This results in a higher extraction efficiency of the air entrapped. In fully clathrated ice an efficiency of at least 90 % is reached which is significantly higher than the performance of most other principles (50 %–80 %). The fine pulverisation also leads to a relatively small difference between the probability to extract the air from small enclosures and the probability to extract the air from large enclosures. Therefore, climatic CO_2 variations can also be detected in the BCTZ of ice cores with the new CIM. However, a four times higher scatter compared to pure bubble or clathrate ice and an offset in the range of 20 ppmv to the atmospheric concentration limit the use of these data. Sublimation extraction releases 100 % of the trapped air for which reason no offset between the atmospheric and extracted air composition is detected in the BCTZ with this method. Therefore, the sublimation technique offers a complementary method for CO_2 measurements within the BCTZ. Compared to the new system, however, currently used sublimation systems need a 6–10 times longer measurement time for the same amount of data points. In addition, the data uncertainty of the latest sublimation system is not (yet) as good as the one of the system presented here. Nevertheless, not all possibilities to optimize the extraction characteristic of the CIM presented here are completely utilised and, hence, potential for improvements in this respect exist.

Besides the increased extraction efficiency, the CIM shows three further advantages compared to previous dry extraction devices: first, no mechanical friction occurs within the new device due to the use of the magnetic bearing technology of Levitronix. Second, contamination with ambient air is negligible since only a small fraction of the inner surfaces is exposed to the ambient air and due to the handling of these surfaces during the potential exposure. Third, the current geometry of the device allows sample weights from a few grams of up to 15 g which does not influence the characteristics of the produced powder and the precision of the system. The device could be modified to accommodate samples of up to 40 g. Therefore, this new dry extraction device may also be used for the extraction of other greenhouse gases such as CH_4 and N_2O. Particular interest exists for the more sensitive reconstruction of isotopic ratios of CO_2 where the throughput of samples could be substantially increased with this principle.

With the exception of the cleaning and ice loading of the CIM all other steps follow an automated protocol. This automation, together with higher precision of the gas analytical part and the smaller sample contamination in the CIM, leads to an approximately three times better precision and a two times better accuracy of single measurements compared to the classical cracker system. For most measurements performed on the fully clathrated ice of the TALDICE ice core, 1–2 replicate measurements are made resulting in a data error of about 1.5 ppmv (1σ). This is comparable to the error of the cracker data of the same depth range of about 1.7 ppmv where 3–9 replicates have been measured. The reproducibility with the CIM system in this ice is about 1.1 ppmv which is competitive with the latest development in this field (Ahn et al., 2009: 0.9–1.5 ppmv). This excellent reproducibility further suggests that replicates might not even be necessary in future measurement campaigns on non-BCTZ ice. Under the assumption that future measurement campaigns with this new system do not require replicates, 12–20 data points per day can be produced in contrast to 3–6 with actual cracker systems and to 1–2 with the latest sublimation system.

Acknowledgements. This work is funded by the Swiss National Science Foundation. We thank Levitronix for providing hardware and technical support, the mechanical staff of our institute and in particular R. Walther for the effort put into the hardware of the new dry extraction device, M. Siegrist for contributions to the software, B. Stauffer and J. Schwander for sharing their valuable experience in experimental engineering and S. Eggleston for providing CO_2 data from the sublimation system.

Edited by: P. Werle

References

Ahn, J. and Brook, E. J.: Atmospheric CO_2 and climate on millennial time scales during the last glacial period, Science, 322, 83–85, 2008.

Ahn, J., Brook, E. J., and Howell, K.: A high-precision method for measurement of paleoatmospheric CO_2 in small polar ice samples, J. Glaciol., 55, 499–506, 2009.

Anklin, M., Barnola, J., Schwander, J., Stauffer, B., and Raynaud, D.: Processes affecting the CO_2 concentrations measured in Greenland ice, Tellus B, 47, 461–470, 1995.

Baer, D. S., Paul, J. B., Gupta, M., and O'Keefe, A.: Sensitive absorption measurements in the near-infrared region using off-axis integrated-cavity-output spectroscopy, Appl. Phys. B, 75, 261–265, 2002.

Baumgartner, M., Schilt, A., Eicher, O., Schmitt, J., Schwander, J., Spahni, R., Fischer, H., and Stocker, T. F.: High-resolution interpolar difference of atmospheric methane around the Last Glacial Maximum, Biogeosciences, 9, 3961–3977, doi:10.5194/bg-9-3961-2012, 2012.

Bereiter, B.: Test und Adaption eines kommerziellen IR-Absorptionsanalysegerätes für CO_2-Messungen an polaren Eisbohrkernen, M.S. thesis, Division of Climate- and Environmental Physics, University of Bern, 2007.

Bereiter, B.: Atmospheric CO_2 Reconstructions using Polar Ice Cores: Development of a New Dry Extraction Device and Insights from Highly Resolved Records, Ph.D thesis, Devision of Climate- and Environmental Physics, University of Bern, 2012.

Bereiter, B., Lüthi, D., Siegrist, M., Schüpbach, S., Stocker, T. F. and Fischer, H.: Mode change of millennial CO_2 variability during the last glacial cycle associated with a bipolar marine carbon seesaw, P. Natl. Acad. Sci., 109, 9755–9760, 2012.

Coachman, L. K., Hemmingsen, E., and Scholander, P. F.: Gas Enclosures in a Temperate Glacier, Tellus, 8, 415–423, 1956.

Crosson, E. R.: A cavity ring-down analyzer for measuring atmospheric levels of methane, carbon dioxide, and water vapor, Appl. Phys. B, 92, 403–408, 2008.

Elsig, J.: New insights into the global carbon cycle from measurements of CO_2 stable isotopes: methodological improvements and interpretation of a new EPICA Dome C ice core $\delta^{13}C$ record, Ph.D thesis, Devision of Climate- and Environmental Physics, University of Bern, 2009.

Indermühle, A., Stocker, T. F., Joos, F., Fischer, H., Smith, H. J., Wahlen, M., Deck, B., Mastroianni, D., Tschumi, J., Blunier, T., Meyer, R. and Stauffer, B.: Holocene carbon-cycle dynamics based on CO_2 trapped in ice at Taylor Dome, Antarctica, Nature, 398, 121–126, 1999.

Kawamura, K., Nakazawa, T., Aoki, S., Sugawara, S., Fujii, Y., and Watanabe, O.: Atmospheric CO_2 variations over the last three glacial-interglacial climatic cycles deduced from the Dome Fuji deep ice core, Antarctica using a wet extraction technique, Tellus, 55, 126–137, 2003.

Lehmann, B., Wahlen, M., Zumbrunn, R., and Oeschger, H.: Isotope analysis by infrared laser spectroscopy, Appl. Phys., 13, 153–158, 1977.

LI-COR: LI-7000 CO_2/H_2O-Analyzer Instruction Manual, 3rd Edn., LI-COR, Lincoln, Nebraska 68504, USA, 2005.

Lüthi, D.: Hochauflösende CO_2 Konzentrationsmessungen an antarktischen Eisbohrkernen: Natürliche Variabilität der letzten 800,000 Jahre und Unsicherheiten aufgrund von Prozessen im Eis, Ph.D thesis, Devision of Climate- and Environmental Physics, University of Bern, 2009.

Lüthi, D., Le Floch, M., Bereiter, B., Blunier, T., Barnola, J., Siegenthaler, U., Raynaud, D., Jouzel, J., Fischer, H., Kawamura, K., and Stocker, T. F.: High-resolution carbon dioxide concentration record 650,000–800,000 years before present, Nature, 453, 379–382, 2008.

Lüthi, D., Bereiter, B., Stauffer, B., Winkler, R., Schwander, J., Kindler, P., Leuenberger, M., Kipfstuhl, S., Capron, E., Landais, A., Fischer, H., and Stocker, T. F.: CO_2 and O_2/N_2 variations in and just below the bubble-clathrate transformation zone of Antarctic ice cores, Earth Planet Sc. Lett., 297, 226–233, 2010.

Neftel, A., Oeschger, H., Schwander, J., Stauffer, B., and Zumbrunn, R.: Ice core sample measurements give atmospheric CO_2 content during the past 40'000 yr, Nature, 295, 220–223, 1982.

Parrenin, F., Barnola, J.-M., Beer, J., Blunier, T., Castellano, E., Chappellaz, J., Dreyfus, G., Fischer, H., Fujita, S., Jouzel, J., Kawamura, K., Lemieux-Dudon, B., Loulergue, L., Masson-Delmotte, V., Narcisi, B., Petit, J.-R., Raisbeck, G., Raynaud, D., Ruth, U., Schwander, J., Severi, M., Spahni, R., Steffensen, J. P., Svensson, A., Udisti, R., Waelbroeck, C., and Wolff, E.: The

EDC3 chronology for the EPICA Dome C ice core, Clim. Past, 3, 485–497, doi:10.5194/cp-3-485-2007, 2007.

Raynaud, D., Lipenkov, V., Lemieux-Dudon, B., Duval, P., Loutre, M., and Lhomme, N.: The local insolation signature of air content in Antarctic ice. A new step toward an absolute dating of ice records, Earth Planet Sc. Lett., 261, 337–349, 2007.

Ruth, U., Barnola, J.-M., Beer, J., Bigler, M., Blunier, T., Castellano, E., Fischer, H., Fundel, F., Huybrechts, P., Kaufmann, P., Kipfstuhl, S., Lambrecht, A., Morganti, A., Oerter, H., Parrenin, F., Rybak, O., Severi, M., Udisti, R., Wilhelms, F., and Wolff, E.: "EDML1": a chronology for the EPICA deep ice core from Dronning Maud Land, Antarctica, over the last 150 000 years, Clim. Past, 3, 475–484, doi:10.5194/cp-3-475-2007, 2007.

Schaefer, H., Lourantou, A., Chappellaz, J., Lüthi, D., Bereiter, B., and Barnola, J.: On the suitability of partially clathrated ice for analysis of concentration and $\delta^{13}C$ of palaeo-atmospheric CO_2, Earth Planet Sc. Lett., 307, 334–340, 2011.

Schilt, A., Baumgartner, M., Schwander, J., Buiron, D., Capron, E., Chappellaz, J., Loulergue, L., Schüpbach, S., Spahni, R., Fischer, H., and Stocker, T. F.: Atmospheric nitrous oxide during the last 140'000 years, Earth Planet Sc. Lett., 300, 33–43, 2010.

Schmitt, J., Schneider, R., and Fischer, H.: A sublimation technique for high-precision measurements of $\delta^{13}CO_2$ and mixing ratios of CO_2 and N_2O from air trapped in ice cores, Atmos. Meas. Tech., 4, 1445–1461, doi:10.5194/amt-4-1445-2011, 2011.

Siegenthaler, U., Stocker, T. F., Monnin, E., Lüthi, D., Schwander, J., Stauffer, B., Raynaud, D., Barnola, J., Fischer, H., Masson-Delmotte, V., and Jouzel, J.: Stable carbon cycle-climate relationship during the late Pleistocene, Science, 310, 1313–1317, 2005.

Siegrist, M.: Entwicklung einer automatisierten Messanlage für CO_2 Messungen an polaren Eisbohrkernen, M.S. thesis, Division of Climate- and Environmental Physics, University of Bern, 2011.

Sowers, T. and Jubenville, J.: A modified extraction technique for liberating occluded gases from ice cores, J. Geophys. Res., 105, 29155–29164, 2000.

Stauffer, B. and Oeschger, H.: Gaseous components in the atmosphere and the historic record revealed by ice cores, Ann. Glaciol., 7, 54–59, 1985.

Tschumi, J. and Stauffer, B.: Reconstructing the past atmospheric CO_2 concentration based on ice-core analyses: open questions due to in situ production of CO_2 in the ice, J. Glaciol., 46, 45–53, 2000.

Uchida, T., Miyamoto, A., Shin'Yama, A., and Hondoh, T.: Crystal growth of air hydrates over 720 ka in Dome Fuji (Antarctica) ice cores: microscopic observations of morphological changes below 2000 m depth, J. Glaciol., 57, 1017–1026, 2011.

Zumbrunn, R., Neftel, A., and Oeschger, H.: CO_2 measurements on 1 cm^3 ice samples with an IR laserspectrometer (IRLS) combined with a new dry extraction device, Earth Planet Sc. Lett., 60, 318–324, 1982.